

AD-A253 066

2



MEMORANDUM REPORT BRL-MR-3984

BRL

DTIC
ELECTE
JUL 20 1992
S

**EFFECT OF VARIABLE THERMAL PROPERTIES
ON GUN TUBE HEATING**

**NATHAN GERBER
MARK BUNDY**

JULY 1992

APPROVED FOR PUBLIC RELEASE; DISTRIBUTION IS UNLIMITED.

U.S. ARMY LABORATORY COMMAND

**BALLISTIC RESEARCH LABORATORY
ABERDEEN PROVING GROUND, MARYLAND**

92-19078



92

NOTICES

Destroy this report when it is no longer needed. DO NOT return it to the originator.

Additional copies of this report may be obtained from the National Technical Information Service, U.S. Department of Commerce, 5285 Port Royal Road, Springfield, VA 22161.

The findings of this report are not to be construed as an official Department of the Army position, unless so designated by other authorized documents.

The use of trade names or manufacturers' names in this report does not constitute indorsement of any commercial product.

REPORT DOCUMENTATION PAGE

Form Approved
OMB No. 0704-0188

Public reporting burden for this collection of information is estimated to average 1 hour per response, including the time for reviewing instructions, searching existing data sources, gathering and maintaining the data needed, and completing and reviewing the collection of information. Send comments regarding this burden estimate or any other aspect of this collection of information, including suggestions for reducing this burden, to Washington Headquarters Services, Directorate for Information Operations and Reports, 1215 Jefferson Davis Highway, Suite 1204, Arlington, VA 22202-4302, and to the Office of Management and Budget, Paperwork Reduction Project (0704-0188), Washington, DC 20503.

1. AGENCY USE ONLY (Leave blank)		2. REPORT DATE <p style="text-align: center;">July 1992</p>	3. REPORT TYPE AND DATES COVERED <p style="text-align: center;">Final, September 1991-February 1992</p>	
4. TITLE AND SUBTITLE <p style="text-align: center;">Effect of Variable Thermal Properties on Gun Tube Heating</p>			5. FUNDING NUMBERS <p style="text-align: center;">PR: 1L162618AH80</p>	
6. AUTHOR(S) <p style="text-align: center;">Nathan Gerber and Mark Bundy</p>				
7. PERFORMING ORGANIZATION NAME(S) AND ADDRESS(ES)			8. PERFORMING ORGANIZATION REPORT NUMBER	
9. SPONSORING / MONITORING AGENCY NAME(S) AND ADDRESS(ES) <p style="text-align: center;">U.S. Army Ballistic Research Laboratory ATTN: SLCBR-DD-T Aberdeen Proving Ground, MD 21005-5066</p>			10. SPONSORING / MONITORING AGENCY REPORT NUMBER <p style="text-align: center;">BRL-MR-3984</p>	
11. SUPPLEMENTARY NOTES				
12a. DISTRIBUTION / AVAILABILITY STATEMENT <p style="text-align: center;">Approved for public release; distribution is unlimited.</p>			12b. DISTRIBUTION CODE	
13. ABSTRACT (Maximum 200 words) <p>Repeated gun firings can steadily elevate the barrel temperature. The firing heat input and the resulting barrel temperature rise depend on the thermal properties of the barrel material. In particular, they depend on the thermal conductivity, specific heat, and mass density. Since conductivity and specific heat depend on barrel temperature, gun barrel heating becomes a nonlinear problem. If the temperature range is large, this temperature dependence can have an effect on the predicted barrel temperature change. We shall show how these effects are modeled by use of a finite difference solution to the one-dimensional (Fourier) equation of heat conduction. Our findings indicate that for the limited number of rounds stowed in a tank, the inclusion of temperature-dependent thermal properties does not have a significant effect on the predicted barrel temperature change.</p>				
14. SUBJECT TERMS <p>gun barrels; finite difference theory; thermal properties; M256 120-mm gun; multiple rounds; tank gun heating</p>			15. NUMBER OF PAGES <p style="text-align: center;">49</p>	
			16. PRICE CODE	
17. SECURITY CLASSIFICATION OF REPORT <p style="text-align: center;">UNCLASSIFIED</p>	18. SECURITY CLASSIFICATION OF THIS PAGE <p style="text-align: center;">UNCLASSIFIED</p>	19. SECURITY CLASSIFICATION OF ABSTRACT <p style="text-align: center;">UNCLASSIFIED</p>	20. LIMITATION OF ABSTRACT <p style="text-align: center;">UJL</p>	

INTENTIONALLY LEFT BLANK.

TABLE OF CONTENTS

	<u>Page</u>
LIST OF FIGURES	v
ACKNOWLEDGMENTS	vii
1. INTRODUCTION	1
2. THE HEATING MODEL	2
3. FORMULATION OF THE PROBLEM	4
3.1 Statement of the Problem	4
3.2 Kirchhoff Transformation	6
3.3 Transformed Radial Coordinate	8
4. INPUT DATA	9
5. FINITE-DIFFERENCE CALCULATION	9
6. ACCURACY CHECK	12
7. COMPUTATIONS	13
8. DISCUSSION	19
9. ADDENDUM: HEAT CONDUCTION EQUATION	20
10. REFERENCES	21
APPENDIX A: STATEMENT OF PROBLEM IN ξ, t VARIABLES	23
APPENDIX B: COEFFICIENTS OF EQUATION 12	27
APPENDIX C: TIMESCALE	31
LIST OF SYMBOLS	35
DISTRIBUTION LIST	37

DQC QUALITY INSPECTED R

Approved For	
REF: USARI	<input checked="" type="checkbox"/>
REF: EAR	<input type="checkbox"/>
Approved and	<input type="checkbox"/>
JAN 11 1964	
By: _____	
Distribution/	
Availability Codes	
(Avail and/or	
Special	
A-1	

INTENTIONALLY LEFT BLANK.

LIST OF FIGURES

<u>Figure</u>	<u>Page</u>
1. Gun Barrel Thermal Conductivity Variation With Temperature	3
2. Gun Barrel Specific Heat Variation With Temperature	3
3. Transverse Cross Section of Gun Barrel	5
4. Gun Barrel Thermal Diffusivity Variation With Temperature	5
5. Kirchhoff Transform, U, vs. Temperature	7
6. Thermal Diffusivity vs. U	8
7a. Bore Gas Temperature Histories at Two Axial Locations	10
7b. Convective Heat Transfer Coefficient Histories at Inner Wall of Gun Barrel at Two Axial Locations	10
8a. Linear and Nonlinear Outer Wall Temperature Histories	14
8b. Detailed Comparison of Linear and Nonlinear Calculations at an Outer Wall Temperature History Peak	14
9a. Comparison of Linear and Nonlinear Inner Wall Temperature Histories at $z = 4.30$ m (Firing Sequence of Table 1)	16
9b. Comparison of Linear and Nonlinear Calculations at an Inner Wall Temperature History Peak at $z = 4.30$ m (Firing Sequence of Table 1)	16
10. Comparison of Linear and Nonlinear Outer Wall Temperature Histories at $z = 4.30$ m (Firing Sequence of Table 1)	17
11. Comparison of Linear and Nonlinear Outer Wall Temperature Histories at $z = 0.615$ m (Firing Sequence of Table 1)	17
12. Comparison of Linear and Nonlinear Inner Wall Temperature Histories at $z = 0.615$ m (Firing Sequence of Table 1)	18
13. Comparison of Linear and Nonlinear Radial Temperature Profiles at $t = 1,000$ s (Firing Sequence of Table 1)	18

INTENTIONALLY LEFT BLANK.

ACKNOWLEDGMENTS

The authors would like to thank Mr. Paul Conroy of the Interior Ballistics Division, Ballistic Research Laboratory (BRL), for supplying us with an interior ballistics prediction of the in-bore gas temperature and heat transfer coefficient, as a function of position and time, for an M256 120-mm gun barrel firing DM13 ammunition. These data were used as input in our computations. We also wish to thank Mr. Joe Cox, Benet Weapons Laboratory, for providing us with the measured values of specific heat as a function of temperature for M256 gun barrel steel. These temperature-dependent data were a critical part of our nonlinear analysis. And finally, we are indebted to Mr. Jim Bradley, Launch and Flight Division, BRL, for his adept skills at programming our mathematical formulation into an efficient FORTRAN code.

INTENTIONALLY LEFT BLANK.

1. INTRODUCTION

Gun tube heating from multiple firings continues to be a subject of concern to ordnance engineers. A number of investigators have modeled the heating. Some recent publications include: Artus and Hasenbein (1989); Chandra and Fisher (1989a, 1989b); Talley (1989a, 1989b); Rapp (1990); Chandra (1990); Gerber and Bundy (1991); and Conroy (1991). In these studies, the thermal conductivity, density, and specific heat of the metal were taken to be constants, and the resulting problems were linear. However, the conductivity and specific heat are, in fact, functions of temperature.

During the heat transfer process from a single gun firing, the temperature of the metal near the bore surface can rise more than 500 K. The specific heat and thermal conductivity will vary significantly over such a large temperature interval. According to Fourier's heat flux principle, we expect an increase in the conductivity with temperature to augment the resulting heat transfer, and hence further increase the temperature over a scenario in which the conductivity is constant. On the other hand, an increase in specific heat with temperature will have the opposite effect—it will tend to diminish the subsequent temperature rise. Thus, it is difficult to discern, a priori, what effect temperature-dependent thermal properties will have on gun tube heating. We propose to answer this question by solving the nonlinear heat transfer problem with a finite difference solution, using the Crank-Nicolson implicit scheme with iteration. Application of the Kirchhoff transformation, described in Section 3, will render the problem more tractable.

We choose to apply the model to gun barrel heating in tank guns, specifically, the 120-mm M256 cannon for the M1A1 tank. A tank gun is ammunition-limited by the onboard stowage restrictions. This imparts an upper limit to the firing-induced barrel temperature change for tank guns that does not hold for unlimited-fire guns, such as small-caliber chain guns or large-caliber artillery guns. Consequently, we do not treat the broadest possible temperature range for all types of guns; nevertheless, our findings cover a substantial temperature span. The findings indicate that the inclusion of temperature dependence in the modeled thermal properties does not have a significant impact on the barrel temperature predictions over the range investigated.

2. THE HEATING MODEL

We shall compute the gun barrel heating for multiple firings by an extension of the model used in Gerber and Bundy (1991). The following assumptions apply here:

(1) Temperature gradients in the axial direction are neglected in comparison to those in the radial direction.

(2) Temperature is axisymmetric in the plane normal to the bore axis. This implies axisymmetric heat input, as well as the neglect of gravity, barrel thickness variation, and other effects that would cause azimuthal dependence.

(3) Feedback of barrel heating to flow in the gun bore is neglected, so that the same bore temperature and convective heat transfer coefficient histories (for a single round) furnish the input data for every round calculated.

(4) Friction heating is neglected.

(5) Thermal expansion of the barrel is not considered to have an effect on the heat transfer process.

(6) The density, ρ , of the gun barrel metal is constant ($= 7,827 \text{ kg/m}^3$).

(7) The thermal conductivity, k , and the specific heat, c_p , of the metal are functions of the temperature, T , as shown in Figures 1 and 2, respectively. (Figure 1 is based on data from the Material Properties Data Center [1973]; Figure 2 is based on data provided by Joseph Cox, Benet Weapons Laboratory [1990].) Also indicated in the figures are the constant values used by the authors for k and c_p in a previous study (Gerber and Bundy 1991): $k = 38.07 \text{ J/(m s K)}$ and $c_p = 469.05 \text{ J/kg K}$. The particular constants chosen are within the range of values spanned in the course of a typical firing scenario.

The abrupt changes in the curve of Figure 2 are associated with the phase transition of steel from a body-centered crystal lattice structure (ferrite) to a face-centered lattice structure (austenite). Even though we adjust the k and c_p to account for phase transition in the conduction equation, we shall not (in this report) further modify the conduction equation to account for the latent heat effects of the phase transition.

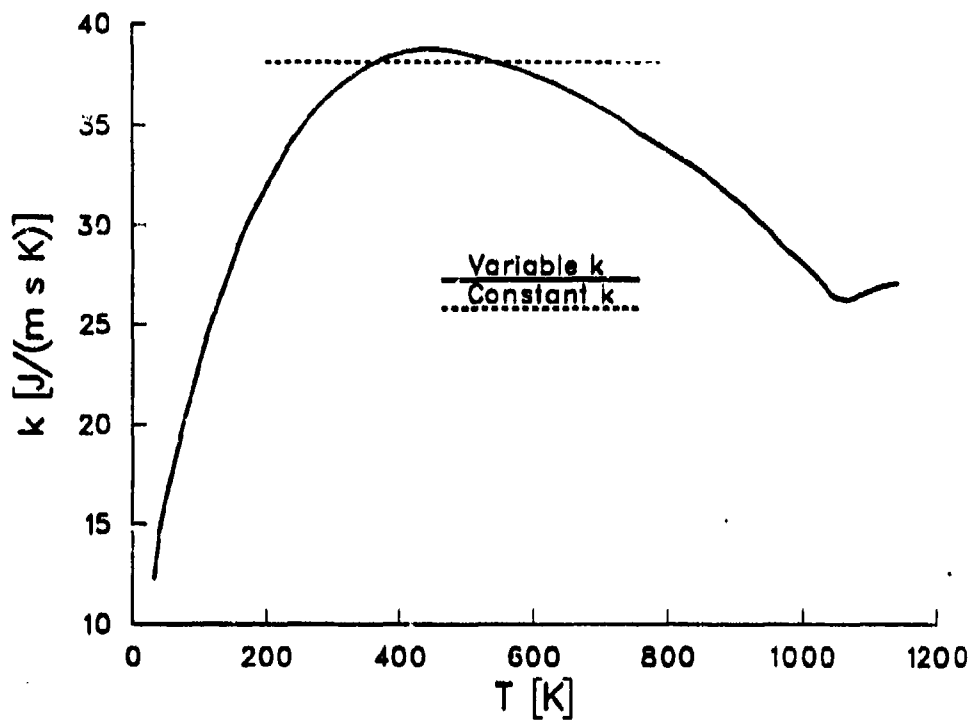


Figure 1. Gun Barrel Thermal Conductivity Variation With Temperature.

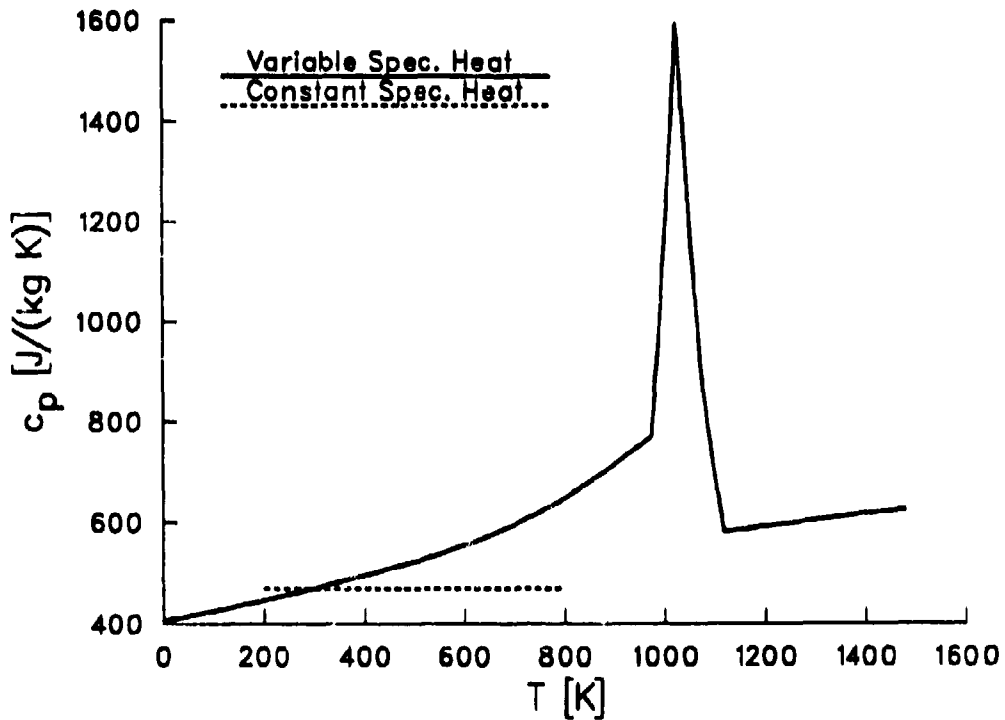


Figure 2. Gun Barrel Specific Heat Variation With Temperature.

3. FORMULATION OF THE PROBLEM

3.1 Statement of the Problem. We state our problem in terms of cylindrical coordinates: r , θ , and z . The radial coordinate, r , is zero on the axis of the gun tube (z -axis), and varies from R_1 to R_0 , the radii of the concentric inner and outer walls, respectively (Figure 3). As implied in Section 2, the azimuthal angle, θ , does not enter the problem. The axial coordinate, z , is taken to be zero at the gun's breech. The barrel temperature, $T(r,z,t)$, where t is time measured from the initiation of the first round, is determined by the following differential equation of heat conduction for a stationary, homogeneous, isotropic solid with no internal heat generation (Özisk 1968, 353, or see ADDENDUM):

$$\rho c_p \partial T / \partial t = \text{div} [k \text{ grad } T] .$$

Under the assumptions made in Section 2, this equation reduces to

$$(1/\alpha) \partial T / \partial t = [\partial^2 T / \partial r^2 + (1/r) \partial T / \partial r] + (dk/dT) (\partial T / \partial r)^2 / k , \quad (1)$$

where $\alpha = k/(\rho c_p)$ is the thermal diffusivity, now a function of T as shown in Figure 4.

The initial and boundary conditions do not change in form from those for constant properties. Let T_∞ designate the ambient temperature of the atmosphere, assumed to be constant. The initial condition is

$$T(r) = T_\infty , \quad t = 0, R_1 \leq r \leq R_0, (z = \text{const}) . \quad (2)$$

The boundary condition at the inner wall is Newton's law of cooling:

$$-k \partial T / \partial r = h_g (T_g - T) , \quad r = R_1 , t > 0 (z = \text{const}) , \quad (3)$$

where $T_g(t,z)$ is the cross-sectional average temperature of the flow in the bore, and $h_g(t,z)$ is the coefficient of heat transfer between the gas-particle mixture in the bore and the inner wall of the barrel. $T_g(t,z)$ and $h_g(t,z)$ are known from interior ballistic computations and thus constitute input.

The boundary condition at the outer wall, which includes both convective and radiative cooling (Özisk 1968; Equations 1-28 and 8-137c), is

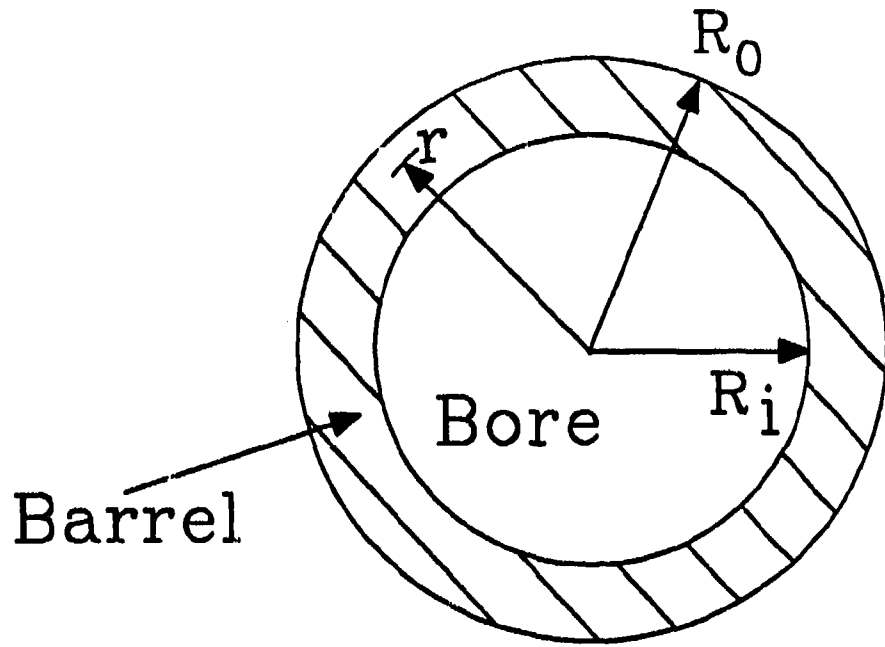


Figure 3. Transverse Cross Section of Gun Barrel.

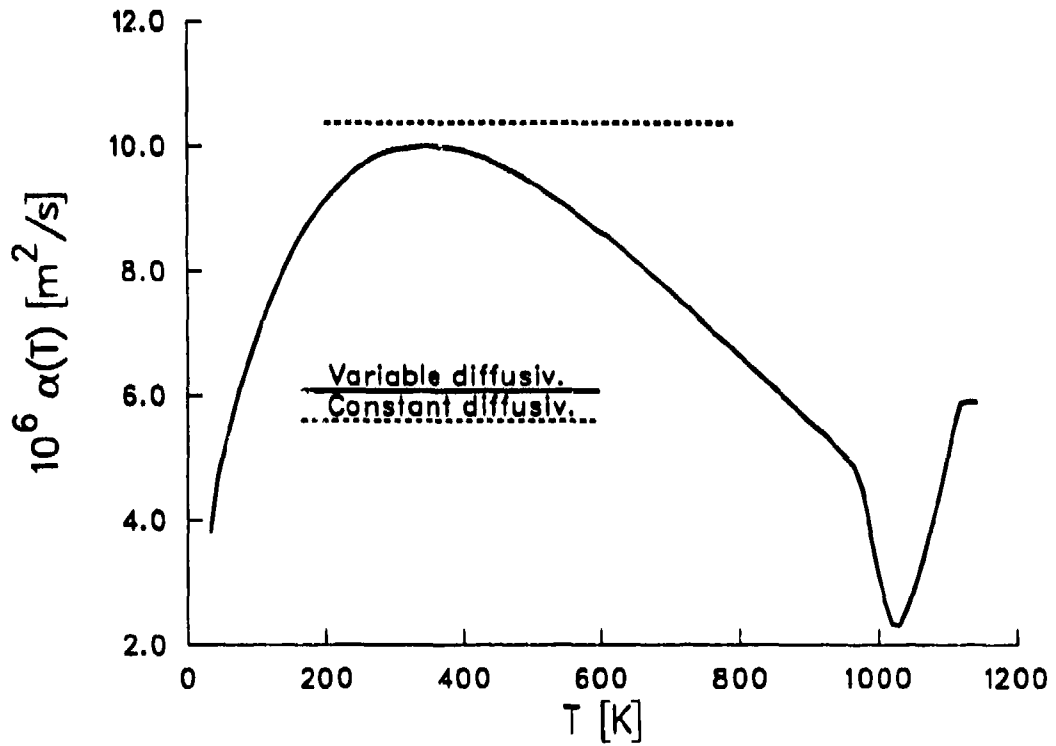


Figure 4. Gun Barrel Thermal Diffusivity Variation With Temperature.

$$-k \frac{\partial T}{\partial r} = h_{\infty} (T - T_{\infty}) + F\sigma (T^4 - T_{\infty}^4) \quad r = R_o, t > 0 (z = \text{const}), \quad (4)$$

where $h_{\infty} = h_{\infty}(z)$ is the coefficient of convective heat transfer between the barrel wall and the surrounding atmosphere. F is the radiation interchange factor between the barrel outer wall and the environment (in our case, assumed = 0.95), and σ is the Stefan-Boltzmann constant [$= 5.669 \times 10^{-8} \text{ J}/(\text{m}^2 \text{ s K}^4)$].

3.2 Kirchhoff Transformation. Equations 1, 3, and 4 show that the heat conduction problem is nonlinear in T . Introducing the Kirchhoff transformation (Özisik 1968, 353; Boley and Weiner 1960, 141),

$$U(T) = \int_{T_1}^T [k(\tau)/k_1] d\tau, \quad (5)$$

will simplify the conduction equation and boundary conditions. U has the dimensions of temperature. Here, T_1 is an arbitrarily chosen lower integration limit, namely, a data point in our table for k ; $T_1 = 33.4512 \text{ K}$ and $k_1 = k(T_1) = 12.801 \text{ J}/(\text{m s K})$. We shall solve the problem posed in terms of U and then evaluate $T(U)$ from the inverse of the Kirchhoff transformation.

The variable coefficients $k(T)$, $c_p(T)$, and $\alpha(T)$ are available in tabular form. For a particular argument, the function value is evaluated by 3-point interpolation. $U(T)$ is obtained in tabular form by numerical integration; it is the solid curve in Figure 5.* The problem now has the form

$$(1/\alpha) \frac{\partial U}{\partial t} = \frac{\partial^2 U}{\partial r^2} + (1/r) \frac{\partial U}{\partial r} \quad (6a)$$

$$-k_1 \frac{\partial U}{\partial r} = h_g [T_g - T(U)] \quad r = R_i, t > 0 \quad (6b)$$

$$-k_1 \frac{\partial U}{\partial r} = h_{\infty} (T - T_{\infty}) + F\sigma (T^4 - T_{\infty}^4) \quad r = R_o, t > 0 \quad (6c)$$

$$U = U_{\infty} = U(T_{\infty}) \quad t \leq 0, R_i \leq r \leq R_o \quad (6d)$$

* It was necessary to extend the tables of k and U in Figures 1 and 5 by extrapolation to higher temperatures (2,000 K) because of extremely high surface temperatures attained briefly in the chamber.

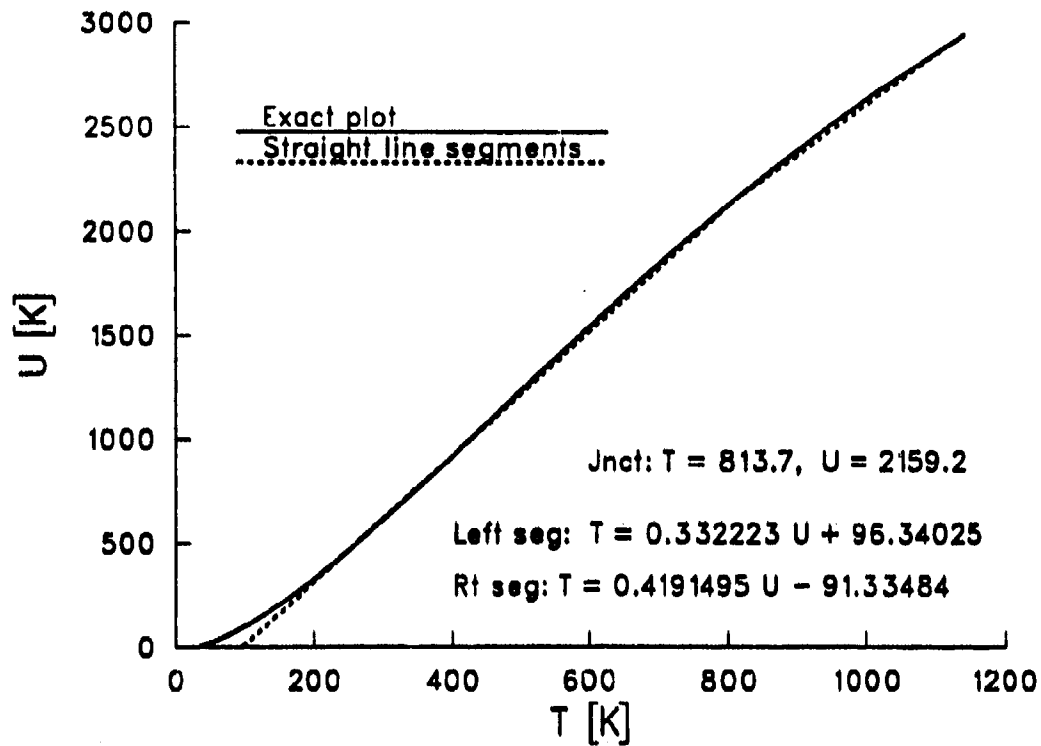


Figure 5. Kirchhoff Transform, U, vs. Temperature.

The diffusivity, $\alpha = \alpha[T(U)]$, is a function of U, shown in Figure 6; thus, Equation 6a is still nonlinear. However, the highly nonlinear term containing k and its derivative no longer appears. In order to render the finite-difference algorithms for the boundary conditions linear, we introduce two linearizing approximations.

For the first approximation, let t^m denote the m th time step of the calculation, when the solution is known, and t^{m+1} the next time step, when the solution is to be found. At $r = R_0$ we assume that

$$| T(R_0, t^{m+1}) - T(R_0, t^m) | \ll T(R_0, t^m).$$

Then Equation 6c, at $r = R_0$ and $t = t^{m+1}$, is approximated by

$$k_1 \partial U / \partial r + [h_{\infty} + 4F\sigma (T^m)^3] T^{m+1} = h_{\infty} T_{\infty} + F\sigma [T_{\infty}^4 + 3(T^m)^4]. \quad (7)$$

This is a reasonable approximation because the temperature changes most slowly at the outer wall; furthermore, the time increment $\Delta t = t^{m+1} - t^m$ can be decreased to ensure the above inequality condition.

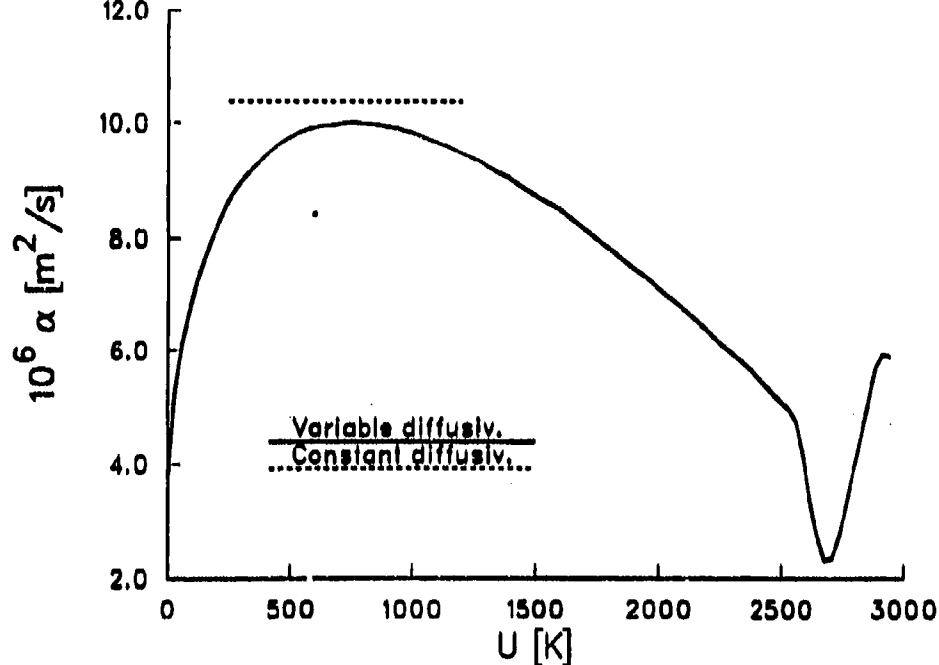


Figure 6. Thermal Diffusivity vs. U.

The second approximation consists of expressing the T in Equations 6b and 7 as a linear function of U . The dashed curve in Figure 5 shows that this can be accomplished with reasonable accuracy by the use of two straight line segments. Thus $T = b_1 U + b_2$, where

$$b_1 \begin{cases} = 0.332223 & \text{if } U \leq 2,159.2 \\ = 0.4191495 & \text{if } U > 2,159.2 \end{cases} \quad b_2 \begin{cases} = 96.34025 & \text{if } U \leq 2,159.2 \\ = -91.33484 & \text{if } U > 2,159.2 \end{cases} .$$

Since it is necessary to choose one of the two line segments a priori at time $t = t^{m+1}$, we base the choice on the U (inner or outer wall) at time $t = t^m$.

3.3 Transformed Radial Coordinate. We introduce a transformation $r = r(\xi)$ for $0 \leq \xi \leq 1$ (Gerber and Bundy 1991) so that the constant increment $\Delta\xi$ will cluster the nodal points closely together near the inner wall, where T and U gradients are the largest. We define the transformation in the following two steps:

$$\begin{cases} \zeta(\xi) = \gamma\xi + (1-\gamma)\xi^\beta, & (0 \leq \gamma \leq 1, \beta > 2), \\ r = D\zeta + R_1, \end{cases} \quad (8)$$

where $D = R_o - R_i$, and γ and β are chosen constants. We chose values of $\gamma = 0.092$ and $\beta = 2.25$, which provided a suitable distribution of nodes. Note that $r = R_i, R_o$ correspond to $\xi = 0, 1$, respectively. The actual computations are then carried out in the ξ, t space; a restatement of the problem in ξ and t is provided in Appendix A.

4. INPUT DATA

A detailed discussion of the input to the computations is given in Gerber and Bundy (1991). Briefly, however, T_g is computed at chosen stations along the bore from the NOVA code (Gough 1980) and h_g is computed from the Veritay code (Chandra and Fisher 1989a, 1989b), which uses T_g and other NOVA variables to determine h_g by the method of Stratford and Beavers (1961).

Figures 7a and 7b show representative T_g and h_g histories at two stations on a 120-mm M256 gun barrel. It is seen that T_g and h_g remain constant until the base of the projectile passes the given station at time $t = t_i$. At this time, these variables rise suddenly to a peak, then they decrease gradually, with h_g decaying significantly faster than T_g .

All the computations reported here were performed for a 120-mm M256 tank gun firing a DM13 round.* The density of the gun barrel metal is taken to be $\rho = 7,827.0 \text{ kg/m}^3$. The thermal conductivity and specific heat are supplied by tables that are plotted in Figures 1 and 2, respectively. The value for $h_{\infty} = 6.0 \text{ J/(m}^2 \text{ s K)}$ was obtained from experiments conducted by Bundy on a shrouded M256 barrel.

5. FINITE-DIFFERENCE CALCULATION

For the finite-difference calculations, the interval $0 \leq \xi \leq 1$ (corresponding to $R_i \leq r \leq R_o$) is divided by equally spaced nodal (or grid) points into NI subintervals. The constant ξ increment is $\Delta\xi = 1/NI$, and the location of the nodes is given by $\xi_j = (j - 1) \Delta\xi$ ($j = 1, 2, \dots, NI + 1$). Derivatives at node j are approximated as follows:

* Table 1 of Gerber and Bundy (1991) describes the shape of the gun barrel.

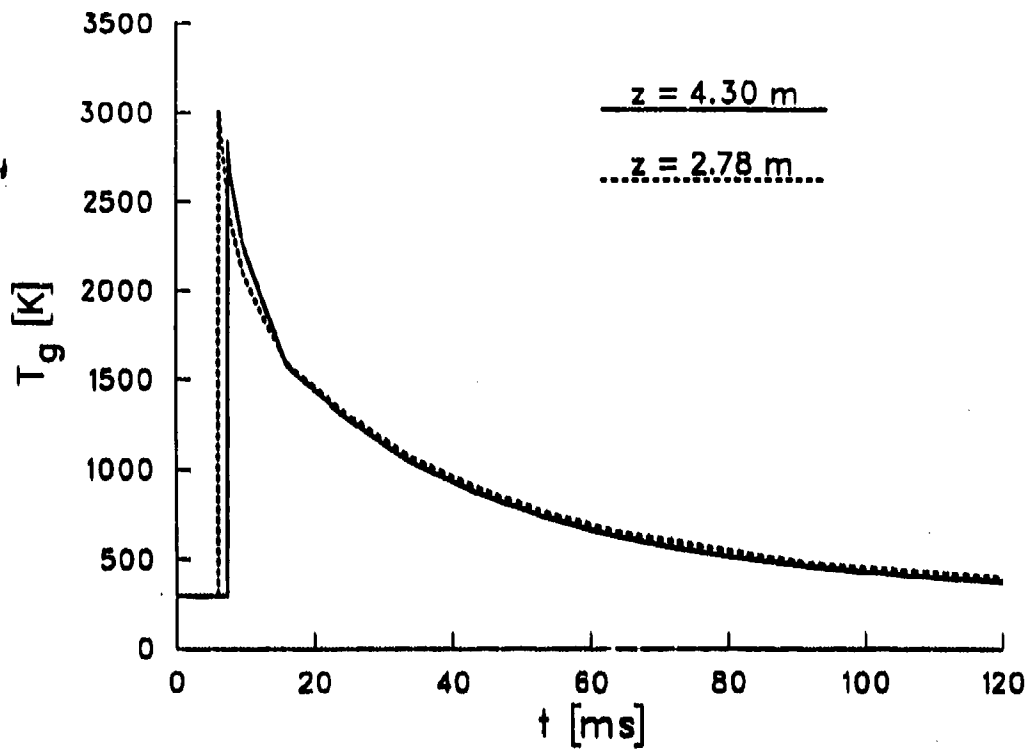


Figure 7a. Bore Gas Temperature Histories at Two Axial Locations.

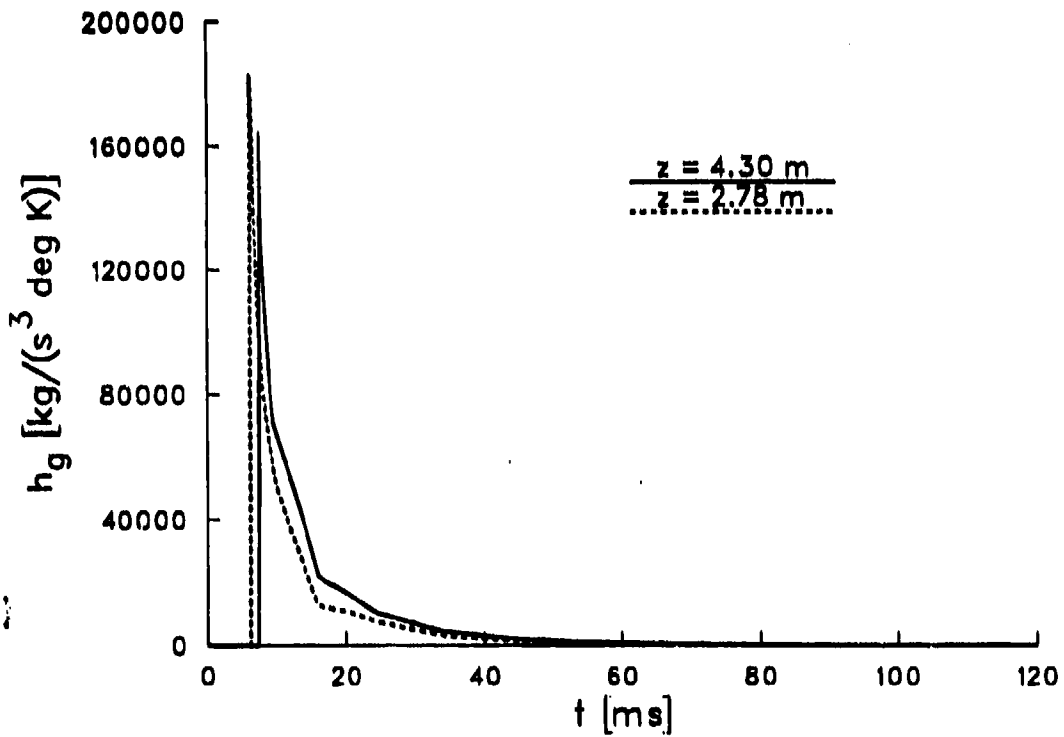


Figure 7b. Convective Heat Transfer Coefficient Histories at Inner Wall of Gun Barrel at Two Axial Locations.

$$(\partial U / \partial \xi)_j = (-3 U_j + 4 U_{j+1} - U_{j+2}) / (2 \Delta \xi) \quad (j = 1) \quad (9a)$$

$$(\partial U / \partial \xi)_j = (U_{j+1} - U_{j-1}) / (2 \Delta \xi) \quad (j = 2, \dots, NI) \quad (9b)$$

$$(\partial U / \partial \xi)_j = (U_{j-2} - 4 U_{j-1} + 3 U_j) / (2 \Delta \xi) \quad (j = NI + 1) \quad (9c)$$

$$(\partial^2 U / \partial \xi^2)_j = (U_{j-1} - 2 U_j + U_{j+1}) / (\Delta \xi)^2 \quad (j = 2, \dots, NI). \quad (9d)$$

If we let the time increment be $\Delta t = t^{m+1} - t^m$, then, in the Crank-Nicolson scheme employed here (Özisk 1968, 402) to obtain the solution at time $t = t^{m+1}$ ($j = 2, \dots, NI$),

$$(U_j^{m+1} - U_j^m) = (\Delta t / 2) [(\partial U / \partial t)^m + (\partial U / \partial t)^{m+1}]_j \quad (10)$$

By Equation A-4a, Equation 10 becomes

$$U_j^{m+1} - (\Delta t / 2) H_j^{m+1} = U_j^m + (\Delta t / 2) H_j^m, \quad (11)$$

where

$$H = (\alpha / D^2) [f_1(\xi) \partial^2 U / \partial \xi^2 + f_2(\xi) \partial U / \partial \xi],$$

and $f_1(\xi)$ and $f_2(\xi)$ are defined in Equations A-3.

The finite-difference approximations to the equations and boundary conditions are produced by substituting the derivative approximations of Equation 9 into Equations 11, A-4b, and A-4c, and then collecting the terms. The following set of equations for U_j^{m+1} may then be written:

$$\sum_{j=1}^{NI+1} A_{nj} U_j^{m+1} = d_n \quad (n = 1, 2, \dots, NI+1). \quad (12)$$

The coefficients A_{nj} and d_n are given in Appendix B. The d_n 's involve U values for the previous timestep $t = t^m$. In most cases, we have used $NI = 100$.

The coefficients A_{nj} ($j = 2, \dots, NI$) are linear functions of $\alpha(U)$ in Equations (B-3) in Appendix B, and are not predetermined constants. A successive approximation procedure is used to solve Equation 12. First, an initial estimate is made for the α 's, e.g., $(\alpha_j^{m+1})^{1st} = \alpha_j^m$, which are known. These α 's, when substituted into the A_{nj} 's, make Equation 12 a linear system, which is solved for $(U_j^{m+1})^{1st}$ by a standard FORTRAN routine. The next α approximation is $(\alpha_j^{m+1})^{2nd} = \alpha[(U_j^{m+1})^{1st}]$. Then $(U_j^{m+1})^{2nd}$ is the solution to Equation 12 when the $(\alpha_j^{m+1})^{2nd}$ are substituted into the A_{nj} 's; and $(\alpha_j^{m+1})^{3rd} = \alpha[(U_j^{m+1})^{2nd}]$. This procedure is repeated until convergence is obtained; i.e.,

$$|(U_j^{m+1})^{(k+1)th} - (U_j^{m+1})^{kth}| < C_{conv} \quad (j = 1, 2, \dots, NI + 1),$$

where C_{conv} is a chosen arbitrarily small positive constant. Three iterations have been required, on the average, for our calculations.

The computer program contains a subroutine prescribing Δt as a function of t within a firing cycle (see Appendix C). The Δt is made sufficiently small early in the cycle to resolve the highly transient phenomena; then it is increased to minimize computation time. The Crank-Nicolson method is stable for all values of Δt , and there are no restrictions on the relative sizes of Δt and Δz .

After the problem is solved for U , T is found by inverting the Kirchhoff transformation. This step is accomplished by applying three-point interpolation in the stored T , U table.

6. ACCURACY CHECK

The condition of energy balance can be employed as an accuracy check. We define two integral functions: (1) Q_F = net energy per unit length that has entered and exited the barrel since $t = 0$, and (2) Q_b = change in barrel heat content per unit length since $t = 0$.

$$Q_F = 2\pi R_i \int_0^1 h_g(\tau) [T_g(\tau) - T(R_i, \tau)] d\tau - 2\pi R_o \int_0^1 h_w [T(R_o, \tau) - T_w] d\tau \\ - 3.5619 \times 10^{-7} FR_o \int_0^1 [(T(R_o, \tau))^4 - T_w^4] d\tau \quad J/m \quad (13)$$

$$Q_b = 2 \pi \rho \int_{R_1}^{R_0} \left[\int_{T_m}^{T(r)} c_p(\bar{T}) d\bar{T} \right] r dr \quad J/m \quad (14)$$

A necessary, but not sufficient, condition for accuracy is that $Q_b = Q_r$ at each time step.

7. COMPUTATIONS

Computations were performed to determine the heating of a 120-mm M256 gun tube firing DM13 rounds. We chose just two of the many possible firing scenarios. The first chosen firing sequence consisted of 16 rounds at 40-s intervals, followed by 5 rounds at 30-s intervals. Figure 8a compares the two outer wall temperature histories at $z = 4.30$ m, about 1 m from the muzzle. At the end of the firing sequence ($t = 780$ s) there is a 3.8 K discrepancy between the two computations. This represents about 2.6% of the total outer wall barrel temperature change (total temperature change is defined as $T[t] - T_m$). A full-scale plot in T vs. t at the inner wall would not reveal the differences between linear and nonlinear output. Figure 8b shows a greatly magnified picture of the histories at one of the inner wall temperature peaks, where the discrepancy maxima occur. The difference at this point is about 25 K, or about 3.4% of the inner wall barrel temperature change.

The main comparisons were made for our second firing sequence, namely, the one shown in Table 1, which is almost identical to Scenario #2 in Table 1 of Artus and Hasenbein (1989). (Our final burst is seven rounds; that of Scenario #2 is six rounds.) This scenario represents the case where all the M1A1 tank-stowed ammunition is fired as fast as possible, with two intermediate cooldown periods corresponding to accessing different ammunition storage compartments. We have computed the change for 41 rounds, whereas the M1A1 tank stows 40 rounds. Also, we have assumed that all 41 rounds are DM13 (kinetic energy [KE] rounds), whereas in actuality the M1A1 stores a mix of KE and HEAT (high-explosive antitank) rounds.

The simulations were performed at two locations on the barrel, 4.30 m and 0.615 m from the breech, for a high and a low ambient temperature: 322 K (120° F) and 233 K (-40° F), respectively. These two locations correspond to positions where the barrel is relatively thin and thick, respectively. The two ambient temperatures correspond to frequently used Army hot and cold testing conditions. The initial gun barrel temperature was the same as that of the surroundings.

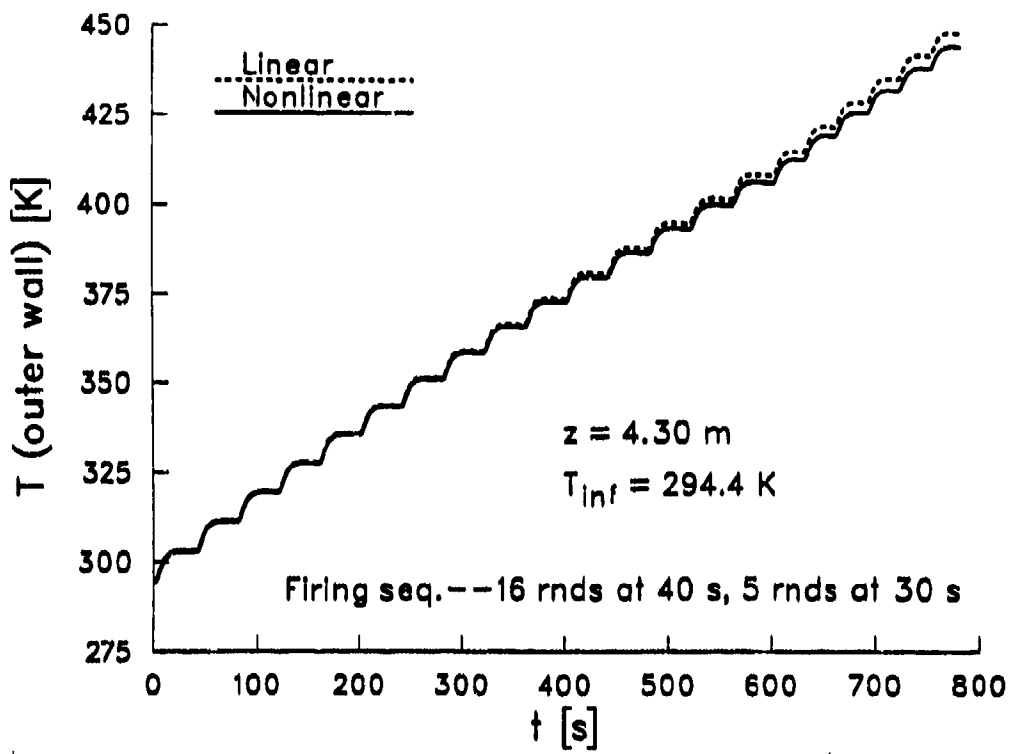


Figure 8a. Linear and Nonlinear Outer Wall Temperature Histories.

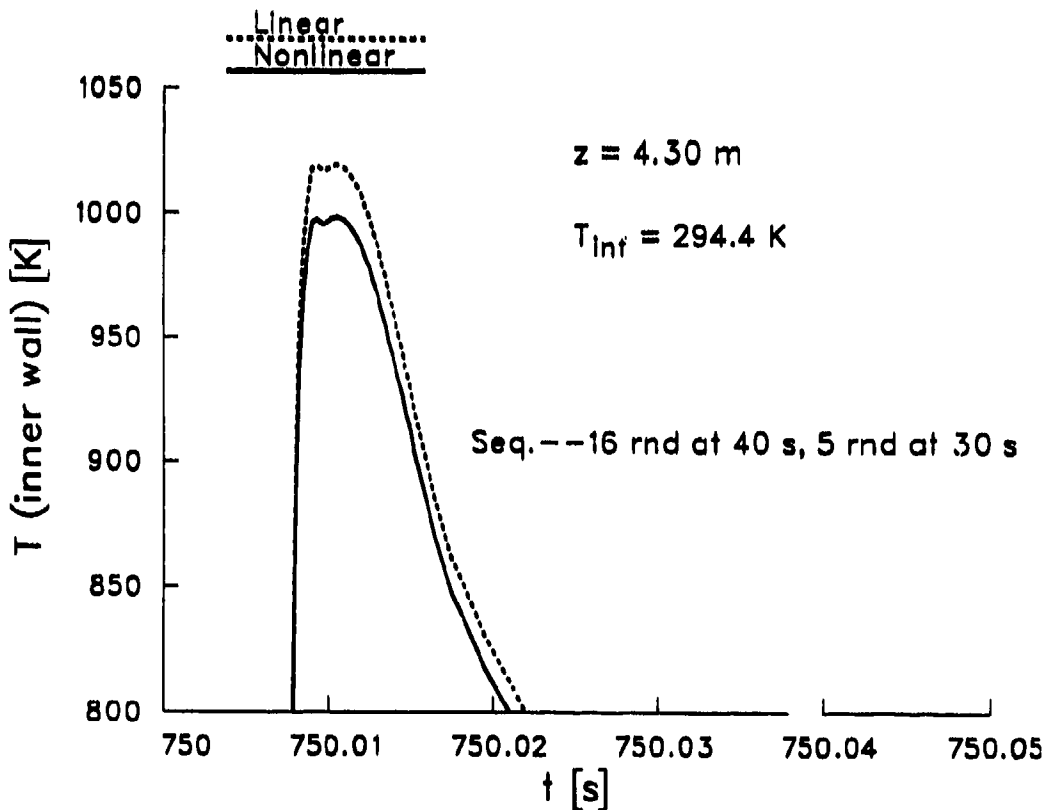


Figure 8b. Detailed Comparison of Linear and Nonlinear Calculations at an Outer Wall Temperature History Peak.

Table 1. Firing Sequence

- | |
|--|
| <ol style="list-style-type: none">1. 17 rounds at 7 rounds/min2. 5 min cool down3. 17 rounds at 7 rounds/min4. 5 min cool down5. 7 rounds at 7 rounds/min6. Cool down |
|--|

Figure 9a presents a comparison of the two inner wall heating predictions at $z = 4.30$ m for $T_{\infty} = 322$ K. (For convenience, $T(R_i)$ has been truncated at 600 K.) The largest difference occurs at the end of each firing burst; at $t = 1,000$ s, for example, the evaluations differ by about 4.8% of the total temperature change, similar to the results from our first firing sequence. Figure 9b shows a greatly magnified picture at one of the temperature peaks. The relative difference between maximum values is about 3.3% of the total temperature change.

In Figure 10, the outer wall temperature calculations are compared for the two ambient temperatures at $z = 4.30$ m. At $t = 1,000$ s, shortly after the end of the final burst, differences are 4.5% and 2.5% of total temperature change for $T_{\infty} = 322$ K and $T_{\infty} = 233$ K, respectively.

The next two figures show heating results at $z = 0.615$ m, close to the breech, for the scenario of Table 1. In Figure 11, the linear and nonlinear calculations are seen to be almost identical, more so even than at $z = 4.30$ m. However, the inclusion of temperature dependence results in a slightly higher, rather than lower (as in Figure 10), outer wall temperature prediction. Figure 12 depicts the inner wall temperature histories under cold and hot firing conditions; the linear and nonlinear curves are almost coincident, at least for the cooling periods.

Figure 13 shows comparisons for the spatial variation of temperature from inner to outer wall for $T_{\infty} = 233$ K. At $z = 0.615$ m, the barrel thickness is 95 mm, compared to 23 mm at $z = 4.30$ m, and the temperature is not able to equilibrate as thoroughly during the 5-minute cooldown periods as it does at the thinner cross section. This behavior is reflected in the fact that T at the thicker section is still varying significantly from the inner to the outer wall. Also, note that the differences between the linear and nonlinear predictions are noticeably greater for thinner barrel cross sections than for the thicker cross sections.

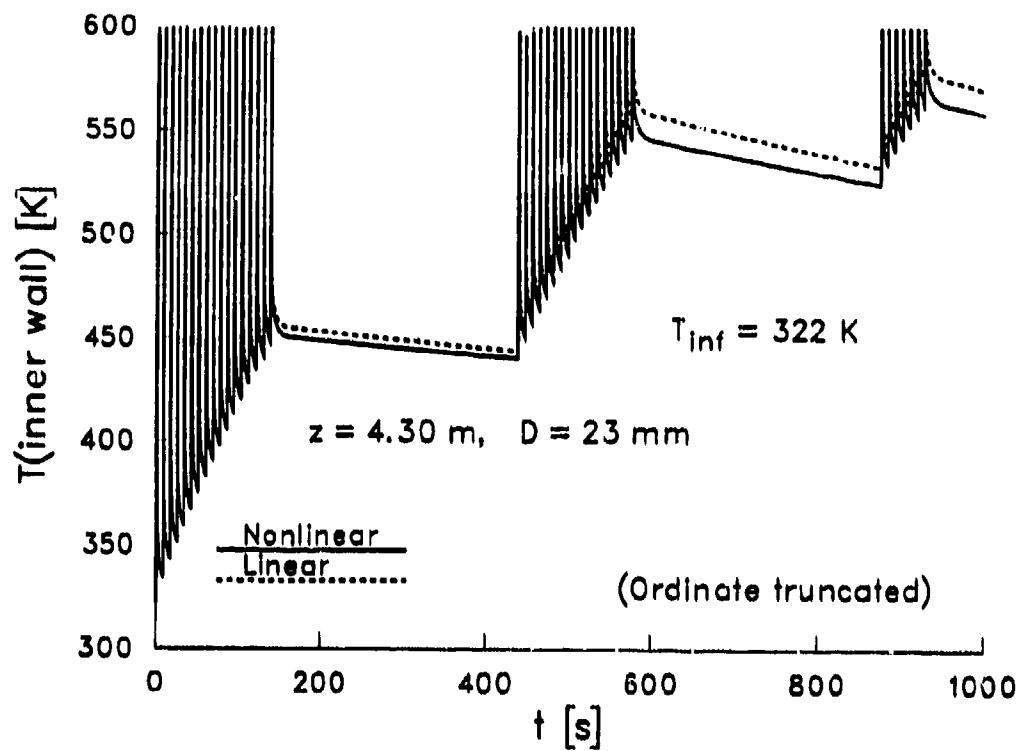


Figure 9a. Comparison of Linear and Nonlinear Inner Wall Temperature Histories at $z = 4.30$ m (Firing Sequence of Table 1).

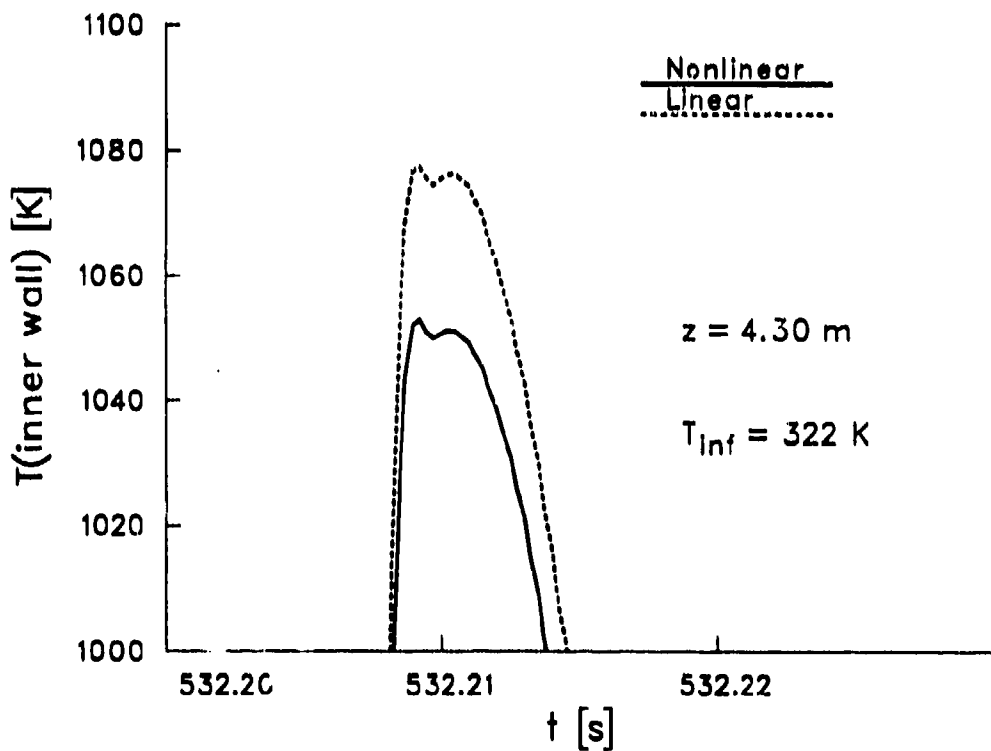


Figure 9b. Comparison of Linear and Nonlinear Calculations at an Inner Wall Temperature History Peak at $z = 4.30$ m (Firing Sequence of Table 1).

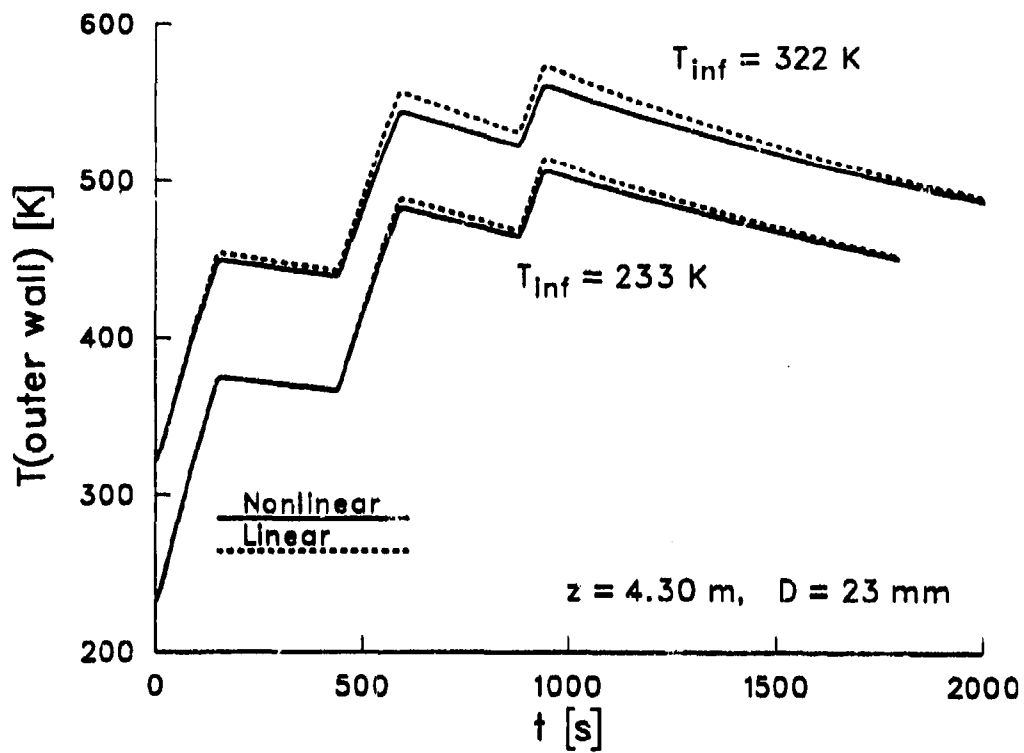


Figure 10. Comparison of Linear and Nonlinear Outer Wall Temperature Histories at $z = 4.30$ m (Firing Sequence of Table 1).

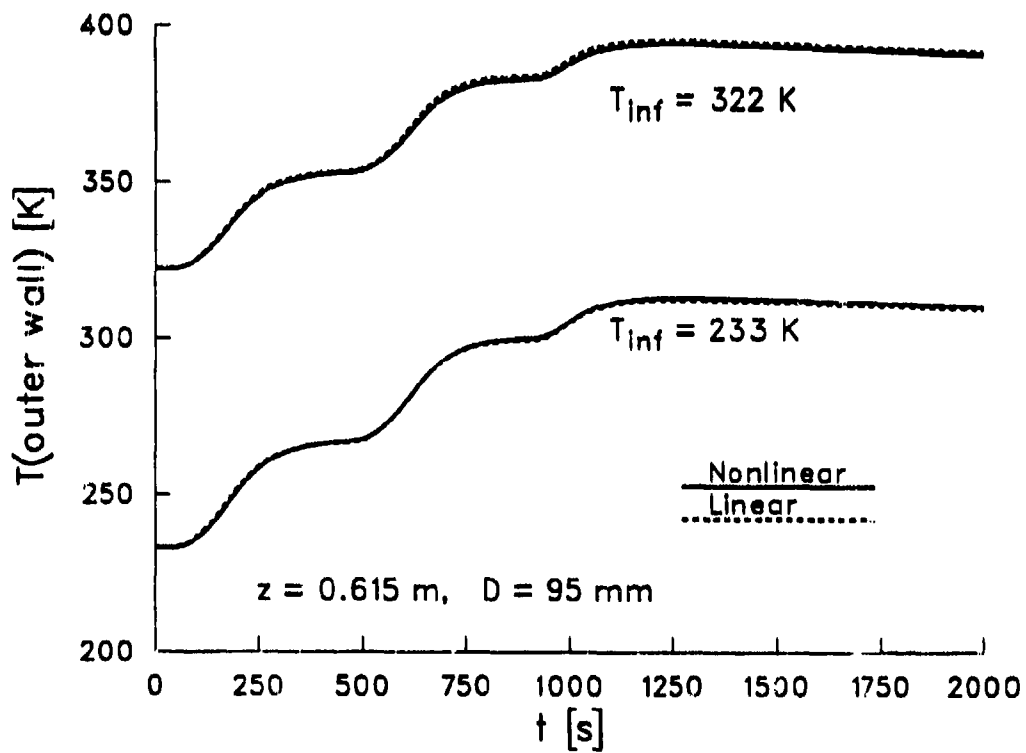


Figure 11. Comparison of Linear and Nonlinear Outer Wall Temperature Histories at $z = 0.615$ m (Firing Sequence of Table 1).

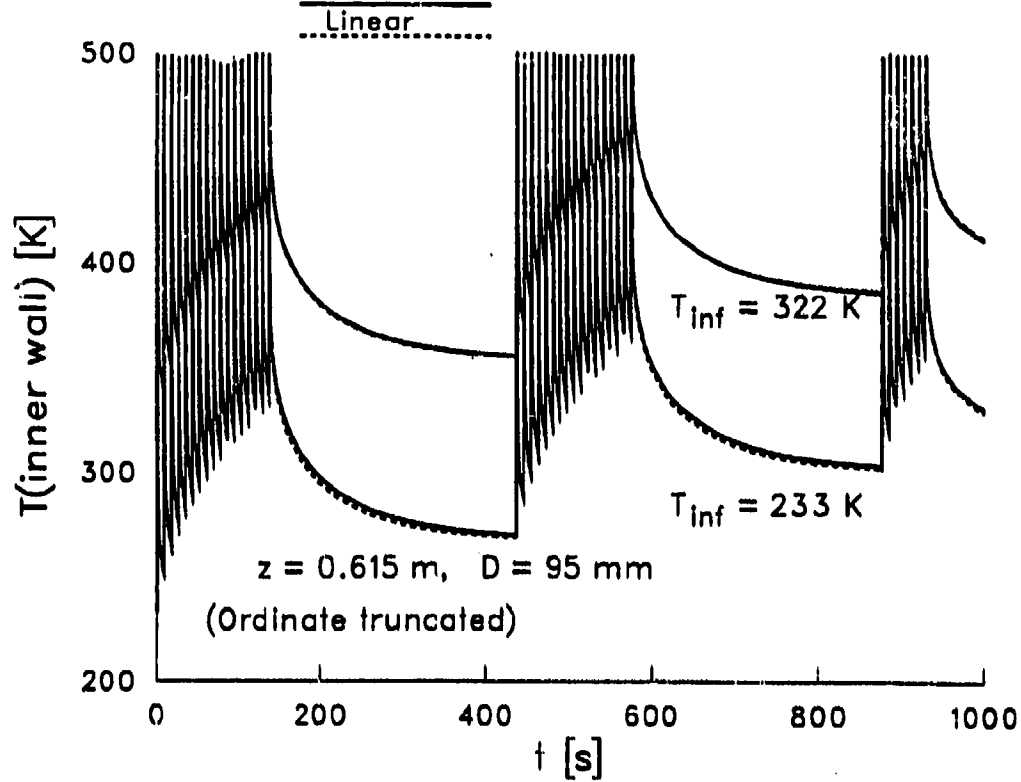


Figure 12. Comparison of Linear and Nonlinear Inner Wall Temperature Histories at $z = 0.615$ m (Firing Sequence of Table 1).

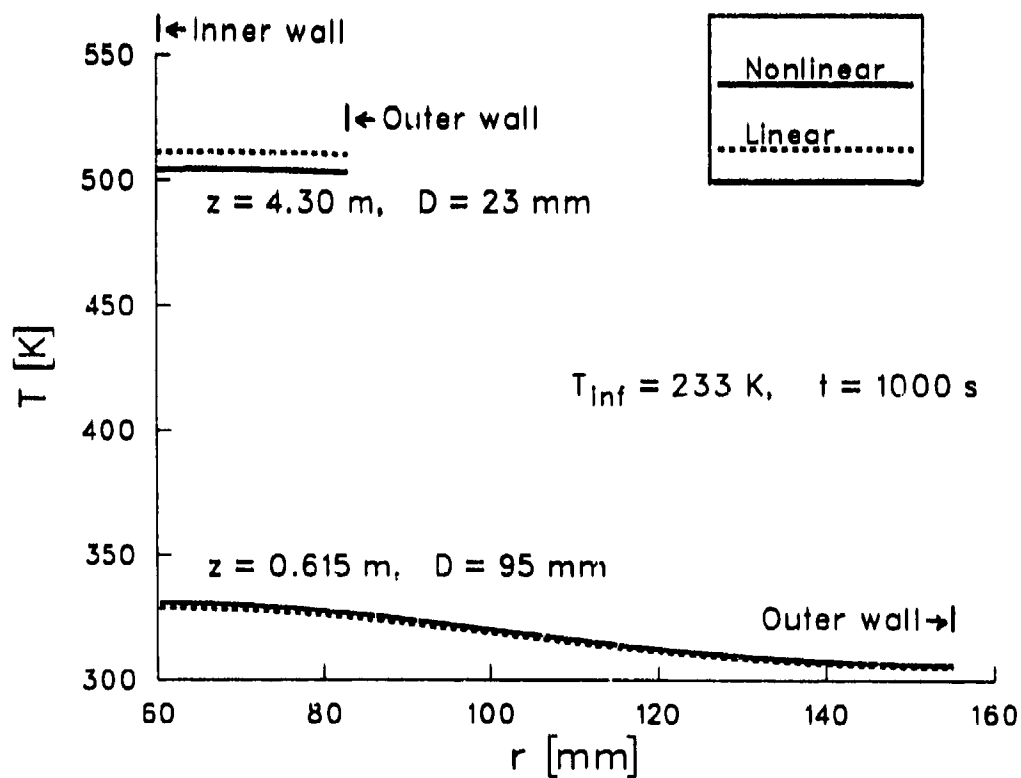


Figure 13. Comparison of Linear and Nonlinear Radial Temperature Profiles at $t = 1.000$ s (Firing Sequence of Table 1).

8. DISCUSSION

This study investigated the "error" introduced into gun barrel heating calculations by assuming constant values of thermal conductivity and specific heat for the metal (linear model) vs. incorporating temperature dependence into these thermal properties (nonlinear model). The constants k and c_p chosen are within the range spanned in the course of a typical firing scenario. Figures 1 and 2 show that the constant values differ significantly from the more accurate temperature-dependent k and c_p at very high temperatures, say above 800 K. For tank guns, however, limitations on the firing rate and number of rounds that can be fired greatly restrict the duration of extremely high temperatures, so that drastic differences need not occur between predictions of the linear and nonlinear models.

It is not feasible to conduct parameter studies for a wide variety of parameters and firing scenarios. We have concentrated on what we believe to be the two cases that should show the greatest difference between these two models: the rapid expenditure of all tank-stowed ammunition under very hot and very cold initial barrel temperatures. We draw several inferences from our limited computer runs:

- (1) Use of variable thermal properties can either increase or decrease the barrel temperature (e.g., Figure 13), depending on the case (that is, on the totality of the computer input parameters, including T_b and h_b histories).
- (2) Differences between linear and nonlinear model temperatures are greater for thinner barrel cross sections (e.g., Figures 9a, 12, and 13). This may be due to the more fundamental fact that thinner cross sections are cycled through a greater temperature range; as a result, the effect of temperature-dependent thermal properties is larger.
- (3) The differences between the outputs of the two models, constant and variable thermal properties, are below 5% for the cases considered. For most tank gun applications, the constant value (or linear) model should be acceptable. In fact, it might be preferred, since it requires roughly one-third of the CPU time of the nonlinear model in each computer run.

9. ADDENDUM: HEAT CONDUCTION EQUATION

In one dimension the heat conduction equation can be understood as follows. For a solid material body, the heat entering per unit area, per unit time through the y-z plane at x, for example, will be given by:

$$Q_{in} = -k \frac{\partial T}{\partial x} \Big|_x .$$

Likewise, the heat leaving through the y-z plane at x+dx will be:

$$Q_{out} = -k \frac{\partial T}{\partial x} \Big|_{x+dx} .$$

The change in internal energy per unit time, per unit volume, will be:

$$\frac{du}{dt} = \frac{Q_{in} - Q_{out}}{dx} = \frac{-k \frac{\partial T}{\partial x} \Big|_x + k \frac{\partial T}{\partial x} \Big|_{x+dx}}{dx} .$$

Expanding the temperature gradient at x + dx about x, retaining terms up to first order in dx, then substituting yields:

$$\frac{du}{dt} = \frac{\partial (k \frac{\partial T}{\partial x})}{\partial x} .$$

From thermodynamics, if the elements boundaries are fixed, then we are assured that $u = u(T)$, and

$$\frac{du(T)}{dt} = \frac{du(T)}{dT} \frac{\partial T}{\partial t} = \rho c_p \frac{\partial T}{\partial t} .$$

Hence, equating the last two expressions, yields:

$$\rho c_p \frac{\partial T}{\partial t} = \frac{\partial (k \frac{\partial T}{\partial x})}{\partial x} .$$

If these arguments were repeated in three dimensions, the results would lead to the heat conduction equation of Section 3.1, viz.:

$$\rho c_p \frac{\partial T}{\partial t} = \nabla \cdot (k \nabla T) .$$

10. REFERENCES

- Artus, B., and R. Hasenbein. "Thermal Study of the 120-mm M256 Cannon Tube." ARCCB-TR-89028, U.S. Army Armament Research, Development, and Engineering Center, Close Combat Armaments Center, Benet Laboratories, Watervliet, NY, October 1989.
- Boley, B., and J. Weiner. Theory of Thermal Stresses. New York: John Wiley and Sons, 1960.
- Chandra, S. "Thermal Response Management of Barrels with XBR-2D." Final Report, Contract DAAA15-88-D-0014, U.S. Army Ballistic Research Laboratory, Aberdeen Proving Ground, MD, December 1990.
- Chandra, S., and E. B. Fisher. "Simulation of Barrel Heat Transfer." Final Report, Contract DAAA15-88-D-0014, U.S. Army Ballistic Research Laboratory, Aberdeen Proving Ground, MD, June 1989a.
- Chandra, S., and E. B. Fisher. "Analysis of 16-inch/50 Gun Chamber Heating." Veritay Report No. C68-1, Naval Ordnance Station, Indian Head, MD, October 1989b.
- Conroy, P. "Gun Tube Heating." BRL-TR-3300, U.S. Army Ballistic Research Laboratory, Aberdeen Proving Ground, MD, December 1991. (AD A243265)
- Gerber, N., and M. Bundy. "Heating of a Tank Gun Barrel: Numerical Study." BRL-MR-3932, U.S. Army Ballistic Research Laboratory, Aberdeen Proving Ground, MD, August 1991. (AD A241136)
- Gough, P. S. "The NOVA Code: A User's Manual - Volume I. Description and Use." IHCR-80-8, Naval Ordnance Station, Indian Head, MD, December 1980.
- Material Properties Data Center. Structural Alloys Handbook. Belfour Stulen, Inc., 1973.
- Özisik, M. N. Boundary Value Problems of Heat Conduction. New York: Dover Publications, Inc., 1968.
- Rapp, J. R. "Gun Tube Temperature Prediction Model." BRL-MR-3844, U.S. Army Ballistic Research Laboratory, Aberdeen Proving Ground, MD, July 1990. (AD B145792)
- Stratford, B. S., and G. S. Beavers. "The Calculation of the Compressible Turbulent Boundary Layer in Arbitrary Pressure Gradient - A Correlation of Certain Previous Methods." Aeronautical Research Council R&M, No. 3207, 1961.
- Talley, J. Q. "Barrel Heating and Erosion in the 105-mm M68A1E3 Gun Tube." Technical Report, Contract DAAA21-86-C-0350 Amendment P00001, U.S. Army Armament Research, Development, and Engineering Center, Picatinny Arsenal, NJ, March 1989a.
- Talley, J. Q. "Barrel Heating and Chrome Plate Adhesion in the 120 mm M256 Gun Tube." Final Report, Contract DAAA21-85-C-0389, U.S. Army Armament Research, Development, and Engineering Center, Picatinny Arsenal, NJ, September 1989b.

INTENTIONALLY LEFT BLANK.

APPENDIX A:
STATEMENT OF PROBLEM IN ξ, t VARIABLES

INTENTIONALLY LEFT BLANK.

We repeat the transformation of Equation 8:

$$\zeta(\xi) = \gamma\xi + (1 - \gamma)\xi^\beta \quad (0 < \gamma \leq 1, \beta > 2) \quad r = D\zeta + R_1. \quad (\text{A-1})$$

Then

$$\begin{aligned} d\zeta/d\xi = \zeta' &= \gamma + \beta(1 - \gamma)\xi^{\beta-1}, & d^2\zeta/d\xi^2 = \zeta'' &= \beta(\beta - 1)(1 - \gamma)\xi^{\beta-2} \\ \zeta'(0) &= \gamma, & \lambda_1 = \zeta'(1) &= \gamma + \beta(1 - \gamma) \\ \lambda_2 = \zeta''(1) &= \beta(\beta - 1)(1 - \gamma). \end{aligned} \quad (\text{A-2})$$

We define f_1 and f_2 :

$$\begin{aligned} f_1 &= 1/(\zeta')^3, \\ f_2 &= (D/\zeta')/(D\zeta + R_1) - \zeta''/(\zeta')^3. \end{aligned} \quad (\text{A-3})$$

The transformed problem for U is

$$\partial U/\partial t = (\alpha/D^2)[f_1(\xi)\partial^2 U/\partial \xi^2 + f_2(\xi)\partial U/\partial \xi] = H(\xi, t) \quad (\text{A-4a})$$

$$\partial U/\partial \xi = [h_1(t)D\gamma/k_1][b_1 U + b_2 - T_1(t)] \quad \text{at } \xi = 0 \quad (\text{A-4b})$$

$$[k_1/(D\lambda_1)]\partial U/\partial \xi + b_1 w_1 U = w_2 - b_2 w_1 \quad \text{at } \xi = 1. \quad (\text{A-4c})$$

where

$$\left. \begin{aligned} w_1 &= h_{\infty} + 4F\sigma(T^{\infty})^3 \\ w_2 &= h_{\infty}T_{\infty} + F\sigma[T_{\infty}^4 + 3(T^{\infty})^4] \end{aligned} \right\} \text{ at } \xi = 1. \quad (\text{A-5})$$

The initial condition is

$$U = U_{\infty} = U(T_{\infty}) \quad t = 0, 0 \leq \xi \leq 1. \quad (\text{A-6})$$

APPENDIX B:
COEFFICIENTS OF EQUATION 12

INTENTIONALLY LEFT BLANK.

We first define $v_1(t)$ and $v_2(t)$:

$$v_1 = 2 \Delta \xi h_p(t) D \gamma / k_1, \quad v_2 = v_1 [b_2 - T_p(t)],$$

where b_1 and b_2 are given in the last paragraph of Section 3.2. Then,

$$\left. \begin{aligned} A_{11} &= -(3 + b_1 v_1), & A_{12} &= 4, & A_{13} &= -1 \\ d_1 &= v_2 \end{aligned} \right\}. \quad (\text{B-1})$$

At the outer wall, where $j = NP = NI + 1$, the coefficients of the boundary condition are determined by the following sequence of formulas:

$$w_1 = h_- + 4 F \sigma (T_{NP}^*)^3$$

$$w_2 = h_- T_- + F \sigma [T_-^4 + 3 (T_{NP}^*)^4]$$

$$\lambda_1 = \gamma + \beta(1 - \gamma)$$

$$q_1 = 2 \Delta \xi w_1 b_1 D \lambda_1 / k_1$$

$$q_2 = 2 \Delta \xi D \lambda_1 (w_2 - w_1 b_2) / k_1$$

$$\left. \begin{aligned} A_{NP, NP-2} &= 1, & A_{NP, NP-1} &= -4, & A_{NP, NP} &= (3 + q_1) \\ d_{NP} &= q_2 \end{aligned} \right\}. \quad (\text{B-2})$$

We next define four functions, p_{1j} , p_{2j} , p_{3j} , and G_j^* for $2 \leq j \leq NI$:

$$p_{1j} = [f_{1j} / (\Delta \xi_j)^2] - [f_{2j} / (2 \Delta \xi_j)]$$

$$p_{2j} = -2 f_{1j} / (\Delta \xi_j)^2$$

$$p_{3j} = [f_{1j}/(\Delta\xi)^2] + [f_{2j}/(2 \Delta\xi)]$$

$$G_j^m = (\alpha_j^m/D^2) [p_{1j} U_{j-1}^m + p_{2j} U_j^m + p_{3j} U_{j+1}^m],$$

where $f_{1j} = f_1(\xi_j)$ and $f_{2j} = f_2(\xi_j)$ are defined in Appendix A. Then

$$A_{j, j-1} = -\Delta t \alpha_j^{m+1} p_{1j}/(2 D^2) \tag{B-3a}$$

$$A_{j, j} = 1 - \Delta t \alpha_j^{m+1} p_{2j}/(2 D^2) \tag{B-3b}$$

$$A_{j, j+1} = -\Delta t \alpha_j^{m+1} p_{3j}/(2 D^2) \tag{B-3c}$$

$$d_j = U_j^m + (\Delta t/2)G_j^m. \tag{B-3d}$$

All other A_{ij} are equal to zero.

APPENDIX C:

TIMESCALE

INTENTIONALLY LEFT BLANK.

Here, time = t' will refer to time within one firing cycle — $t' = 0$ at the beginning of the cycle. Six constants are given: t_d , t_r , t'_1 , t'_2 , $\Delta t'_1$ and $\Delta t'_2$. Here, t_d is the delay time for the rapid rise in T_g and h_g from initial conditions, and t_r is the time between successive firings. The time increment Δt (t') is given by the following function:

$$\Delta t = t_d - \Delta t'_1 \quad 0 \leq t' < t_d - \Delta t'_1$$

$$\Delta t = \Delta t'_1 \quad t_d - \Delta t'_1 \leq t' < t'_1$$

$$\Delta t = C_1 + C_2 t' \quad t'_1 \leq t' < t'_2$$

$$\Delta t = \Delta t'_2 \quad t'_2 \leq t'$$

where

$$C_2 = (\Delta t'_2 - \Delta t'_1) / (t'_2 - t'_1) \text{ and } C_1 = \Delta t'_2 - C_2 t'_2$$

(If $t' + \Delta t'_2 > t_r$, set $\Delta t = t_r - t'$).

A typical set of values of the parameters would be the following:

$$t'_1 = 0.018 \text{ s}, \quad t'_2 = 10.0 \text{ s}, \quad \Delta t'_1 = 0.00025 \text{ s}, \quad \Delta t'_2 = 6.0 \text{ s}.$$

These values were chosen on the basis of experience from many empirical studies made with the numerical parameters.

INTENTIONALLY LEFT BLANK.

LIST OF SYMBOLS

A_{nj}	coefficient in Equation 12 for barrel temperature
b_1, b_2	constants in $T = b_1 U + b_2$, see last paragraph of Section 3.2
$c_p(T)$	specific heat of gun barrel [J/(kg K)]
D	$= (R_o - R_i)$ = thickness of gun barrel [m, mm]
d_n	coefficient in barrel temperature equations, right-hand side of Equation 12
F	radiation interchange factor between barrel outer wall and environment, Equation 4
f_1, f_2	given functions of ξ , Equation A-3
H	function defined in Equation A-4
h_b	heat transfer coefficient - bore to gun barrel [J/(m ² s K)]
h_{∞}	heat transfer coefficient - gun barrel to ambient air [J/(m ² s K)]
j	index indicating radial location of a nodal point ($j = 1$ for inner wall, $j = NP$ for outer wall)
$k(T)$	thermal conductivity of gun barrel [J/(m s K)]
k_1	$k(T_1)$
NI	number of intervals in $R_i \leq r \leq R_o$ and $0 \leq \xi \leq 1$
NP	$= NI + 1$
Q_b	increase in heat content per unit length of barrel since $t = 0$ [J/m]
Q_F	net quantity of heat per unit length that has entered barrel since $t = 0$ [J/m]
R_i, R_o	radial coordinates of inner and outer walls, respectively, of gun barrel [m, mm]
r	radial coordinate in transverse plane [m,mm] ($r = 0$ at axis of gun bore)
T	temperature in gun barrel [K]
T_b, T_{∞}	temperatures in the bore and ambient air, respectively [K]
T_{int}	$= T_{\infty}$
T_1	prescribed lower integration limit in definition of U (Equation 5)

t	time from initiation of first round [s, ms]
t_d	delay time at given z for rapid rise in T_g and h_g [s, ms]
t_r	time interval between two successive rounds [s, ms]
t'	time measured within a firing cycle [s, ms]
$U(T)$	Kirchhoff transformation function, defined in Equation 5 [K]
U_j	$= U(\xi = [j - 1] \Delta\xi)$
U_∞	$= U(T_\infty)$
z	axial coordinate ($z = 0$ at breech) [m]
$\alpha(T)$	$= k/(\rho c_p)$, thermal diffusivity of gun barrel [m^2/s]
β, γ	prescribed constants in coordinate transformation, Equation 8
Δt	computational time increment $= (t^{m+1} - t^m)$ [s]
$\Delta\xi$	$= 1/NI$, constant step size in ξ ($0 \leq \xi \leq 1$)
ζ	$= \gamma \xi + (1 - \gamma) \xi^\beta$
θ	azimuthal coordinate in transverse plane
λ_1, λ_2	$\zeta'(\xi = 1), \zeta'(1)$, defined in Appendix A
ξ	transformed radial variable, Equation 8; independent variable in Equation A-4a
ρ	density of gun barrel metal [kg/m^3]
σ	Stefan-Boltzman constant $= 5.669 \times 10^{-8} J/(m^2 s K^4)$

Superscript

m	index of current time step, when solution is known
$m + 1$	index of next time step, when solution is to be calculated

<u>No. of Copies</u>	<u>Organization</u>	<u>No. of Copies</u>	<u>Organization</u>
2	Administrator Defense Technical Info Center ATTN: DTIC-DDA Cameron Station Alexandria, VA 22304-6145	1	Commander U.S. Army Tank-Automotive Command ATTN: ASQNC-TAC-DIT (Technical Information Center) Warren, MI 48397-5000
1	Commander U.S. Army Materiel Command ATTN: AMCAM 5001 Eisenhower Ave. Alexandria, VA 22333-0001	1	Director U.S. Army TRADOC Analysis Command ATTN: ATRC-WSR White Sands Missile Range, NM 88002-5502
1	Commander U.S. Army Laboratory Command ATTN: AMSLC-DL 2800 Powder Mill Rd. Adelphi, MD 20783-1145	1	Commandant U.S. Army Field Artillery School ATTN: ATSF-CSI Fl Sill, OK 73503-5000
2	Commander U.S. Army Armament Research, Development, and Engineering Center ATTN: SMCAR-IMI-I Picatinny Arsenal, NJ 07806-5000	(Class. only) 1	Commandant U.S. Army Infantry School ATTN: ATSH-CD (Security Mgr.) Fort Benning, GA 31905-5660
2	Commander U.S. Army Armament Research, Development, and Engineering Center ATTN: SMCAR-TDC Picatinny Arsenal, NJ 07806-5000	(Unclas. only) 1	Commandant U.S. Army Infantry School ATTN: ATSH-CD-CSO-OR Fort Benning, GA 31905-5660
1	Director Benet Weapons Laboratory U.S. Army Armament Research, Development, and Engineering Center ATTN: SMCAR-CCB-TL Watervliet, NY 12189-4050	1	WL/MNOI Eglin AFB, FL 32542-5000
(Unclas. only) 1	Commander U.S. Army Rock Island Arsenal ATTN: SMCRI-TL/Technical Library Rock Island, IL 61299-5000	2	<u>Aberdeen Proving Ground</u> Dir, USAMSA ATTN: AMXSY-D AMXSY-MP, H. Cohen
1	Director U.S. Army Aviation Research and Technology Activity ATTN: SAVRT-R (Library) M/S 219-3 Ames Research Center Moffett Field, CA 94035-1000	1	Cdr, USATECOM ATTN: AMSTE-TC
1	Commander U.S. Army Missile Command ATTN: AMSMI-RD-CS-R (DOC) Redstone Arsenal, AL 35898-5010	3	Cdr, CRDEC, AMCCOM ATTN: SMCCR-RSP-A SMCCR-MU SMCCR-MSI
		1	Dir, VLAMO ATTN: AMSLC-VL-D
		10	Dir, USABRL ATTN: SLCBR-DD-T

No. of
Copies Organization

16 Director
Benet Weapons Laboratory
U.S. Army Armament Research,
Development, and Engineering Center
ATTN: SMCAR-CCB-DS, R. Hasenbein
SMCAR-CCB-DA,
J. Neice
G. Carafano
SMCAR-CCB-RA,
B. Pflieg
P. O'Hara
SMCAR-CCB-R',
B. Avitzar
S. Sopok
SMCAR-CCB-RM, M. Withesell
SMCAR-CCB-DI, C. Rinaldi
SMCAR-CCB-RP,
J. Cox
G. Capinialis
SMCAR-CCB-DS, P. Votlis
SMCAR-CCB-DS, C. Andrade
SMCAR-LBD-D, J. Zweig
SMCAR-CCB, L. Johnson
SMCAR-CCB-DA, L. Bennett
Watervliet, NY 12189-4050

2 Director
Benet Weapons Laboratory
U.S. Army Armament Research,
Development, and Engineering Center
ATTN: T. Allen
B. Artus
Watervliet, NY 12189-4050

1 Commander
U.S. Army Tank-Automotive Command
ATTN: SFAE-ASM-AB-SW, Dr. Pattison
Warren, MI 48397-5000

5 Commander
Tank Main Armament System
ATTN: SFAE-AR-TMA,
K. Russell
E. Kopacz
K. Ruben
F. Hildebrand
S. Bernstein
Picatinny Arsenal, NJ 07806-5000

No. of
Copies Organization

2 Commander
U.S. Army Armament Research,
Development, and Engineering Center
ATTN: SMCAR-CCH,
E. Del Coco
K. Pflieger
Picatinny Arsenal, NJ 07806-5000

2 Commander
U.S. Army Armament Research,
Development, and Engineering Center
ATTN: C. Longon
J. DeLabar
Picatinny Arsenal, NJ 07806-5000

1 Director
Weapons Department
U.S. Army Armor School
ATTN: ATSB-WP-ORSA, A. Pomey
Fort Knox, KY 40121-5212

1 Paul Gough Associates, Inc.
ATTN: Dr. Paul S. Gough
1048 South St.
Portsmouth, NH 03801-5423

2 Veritay Technology Incorporated
ATTN: E. B. Fisher
J. Z. Talley
P.O. Box 305
4845 Millersport Highway
East Amhurst, NY 14051

USER EVALUATION SHEET/CHANGE OF ADDRESS

This laboratory undertakes a continuing effort to improve the quality of the reports it publishes. Your comments/answers below will aid us in our efforts.

1. Does this report satisfy a need? (Comment on purpose, related project, or other area of interest for which the report will be used.) _____

2. How, specifically, is the report being used? (Information source, design data, procedure, source of ideas, etc.) _____

3. Has the information in this report led to any quantitative savings as far as man-hours or dollars saved, operating costs avoided, or efficiencies achieved, etc? If so, please elaborate. _____

4. General Comments. What do you think should be changed to improve future reports? (Indicate changes to organization, technical content, format, etc.) _____

BRL Report Number BRL-MR-3984 Division Symbol _____

Check here if desire to be removed from distribution list. _____

Check here for address change. _____

Current address: Organization _____
Address _____

DEPARTMENT OF THE ARMY
Director
U.S. Army Ballistic Research Laboratory
ATTN: SLCBR-DD-T
Aberdeen Proving Ground, MD 21005-5068



NO POSTAGE
NECESSARY
IF MAILED
IN THE
UNITED STATES

OFFICIAL BUSINESS

BUSINESS REPLY MAIL
FIRST CLASS PERMIT No 0001, APG, MD

Postage will be paid by addressee.

Director
U.S. Army Ballistic Research Laboratory
ATTN: SLCBR-DD-T
Aberdeen Proving Ground, MD 21005-5068

